Chapter

Bioconvective Linear Stability of Gravitactic Microorganisms

Ildebrando Pérez-Reyes and Luis Antonio Dávalos-Orozco

Abstract

Interesting results on the linear bioconvective instability of a suspension of gravitactic microorganisms have been calculated. The hydrodynamic stability is characterized by dimensionless parameters such as the bioconvection Rayleigh number R, the gyrotaxis number G, the motility of microorganisms d, and the wavenumber k of the perturbation. Analytical and numerical solutions are calculated. The analytical one is an asymptotic solution for small wavenumbers (and for any motility number) which agrees very well with the numerical solutions. Two numerical methods are used for the sake of comparison. They are a shooting method and a Galerkin method. Marginal curves of R against k for fixed values of d and G are presented along with curves corresponding to the variation of the critical values of R_c and k_c. Moreover, those critical values are compared with the experimental data reported in the literature, where the gyrotactic algae *Chlamydomonas nivalis* is the suspended microorganism. It is shown that the agreement between the present theoretical results and the experiments is very good.

Keywords: bioconvection, hydrodynamic stability, Galerkin method

1. Introduction

Since many years ago, efforts in the experimental and theoretical investigation of the bioconvection phenomenon have been made. These efforts, which lead to the understanding of bioconvective instability, have produced novel and interesting applications. For example, Noever and Matsos [1] proposed a biosensor for monitoring the heavy metal Cadmium based in bioconvective patterns as redundant technique for analysis, a number of researchers [2–6] have been working on the control of bioconvection by applying electrical fields (as in galvanotaxis) to use it as a live micromechanical system to handle small objects immersing in suspensions, Itoh et al. [7, 8] use some ideas of bioconvection in a study for the motion control of microorganism groups like *Euglena gracilis* to manipulate objects by using its phototactic orientation (as in phototaxis), and more recently possibly bioconvection seeded the investigation of Kim et al. [9, 10] for using a feedback control strategy to manipulate the motions of *Tetrahymena pyriformis* as a microbiorobot, among others. Perhaps, further applications on biomimetics [11–13] at the nano- and microscale could be driven by this contribution.

The term bioconvection was first coined by Platt [14] as the spontaneous pattern formation in suspensions of swimming microorganisms. This phenomenon has some similarity with Rayleigh-Benard convection but originates solely from

diffusion and the swimming of the organisms. Reviews about this topic have been published by Pedley and Kessler [15] and Hill and Pedley [16]. Ideas and theories on cellular motility can be found in the book of Murase [17], and the effect of gravity on the behavior of microorganisms is widely explained in the book of Hader et al. [18]. In 1975, Childress et al. [19] presented a model for bioconvection of purely gravitactic microorganisms and their results of a linear theoretical study, and later Harashima et al. [20] studied the nonlinear equations of this model. According to the model of Childress et al. [19], the critical wavenumber at the onset of the instability is always zero. In ordinary particles and colloidal suspensions, the internal degrees of freedom like the internal rotation or spin are important under some geometrical and physical conditions [21, 22]. The case of a suspension of microorganisms is not an exception. For this case, Pedley et al. [23] proposed a gyrotactic model for a suspension of infinite depth. Their model includes the displacement of the gravity from the geometric center in the organisms along their axis of symmetry. Hill et al. [24] performed an analysis of the linear instability of a suspension of gyrotactic microorganisms of finite depth using the model of Pedley et al. [23]. Hill et al. [24] found finite wavenumbers at the onset of the instability, but agreement with the experiment was not good. Later, Pedley and Kessler [25] reported a model for suspensions of gyrotactic microorganisms where account was taken of randomness in the swimming direction of the cells. In a study of the linear instability of the system based on the model of Pedley and Kessler [25], Bees and Hill [26] found disagreement between their theoretical results and the experimental data reported by Bees and Hill [27]. Several experimental investigations of bioconvection have been reported by Loeffer and Mefferd [28] and Fornshell [29], by Kessler [30] and Bees and Hill [27] who take into account the gyrotaxis, by Dombrowski et al. [31] and Tuval et al. [32] who take into account the oxitaxis, and more recently by Akiyama et al. [33] who observed a pattern alteration response characterized by a rapid decrease in the bioconvective patterns. Pattern formation has been observed in cultures of different microorganisms such as *Chlamydomonas nivalis*, *Chlamydomonas reinhardtii*, *Euglena gracilis*, *Bacillus subtilis*, *Paramecium tetraurelia*, and *Tetrahymena pyriformis*.

More recently, investigations have been reported for a semi-dilute suspension of swimming microorganisms where cell–cell interactions are considered [34–38]. On the other hand, Kitsunezaki et al. [39] investigated the effect of oxygen and depth on bioconvective patterns in suspensions with high concentrations of *Paramecium tetraurelia*. Bioconvection is also studied from other points of view in gravitational biology. Interesting results are also available in Refs. [40–42] about the pattern formation in suspensions of *Tetrahymena* and *Chlamydomonas* subject to different gravity conditions. Further results are due to Sawai et al. [43] who investigate the proliferation of *Paramecium* under simulated microgravity, to Mogami et al. [44] who report an investigation of the formed patterns by *Tetrahymena* and *Chlamydomonas* as well as a physiological comparison, to Takeda et al. [45] who give an explanation of the gravitactic behavior of single cells of *Paramecium* in terms of the swimming velocity and swimming direction, to Mogami et al. [46] who present theory and experiments of two mechanisms of gravitactic behavior for microorganisms, and to Itoh et al. [47] who investigate the modification of bioconvective patterns under strong gravitational fields.

This chapter presents interesting results about the bioconvective linear stability of a suspension of swimming microorganisms. Use is made of the equations presented by Ghorai and Hill [48, 49] some years ago. In their approach, Ghorai and Hill [48, 49] used a different dimensionalization scale for the concentration microorganisms which gives distinct meaning to the basic state for the concentration of microorganisms and a bioconvective Rayleigh number defined in terms of the mean cell

concentration. To the authors best knowledge, those equations along with the change in the basic state and Rayleigh number definitions have not been used to determine the linear bioconvective instability in an infinite horizontal fluid layer and to compare the results with experiment. These results were obtained by means of both numerical and analytical techniques. The critical values of the Rayleigh number R_c and the wavenumber k_c, for fixed values of the gyrotaxis number G and the motility of microorganisms d, that characterize the hydrodynamic stability of the system are compared with the experimental data presented in Table I of Bees and Hill [27] and Table II of Bees and Hill [26] where the gyrotactic biflagellate alga *Chlamydomonas nivalis* is used as suspended microorganism. Below, it is shown for the first time that the numerical results have a very good agreement with the experimental data.

The chapter is organized as follows. The governing equations and boundary conditions [48, 49] as well as the basic state can be found in Section 2. Nondimensionalization and linearization of the system of equations is outlined in Section 3. In Section 4, use is made of an asymptotic expansion [50–53] method and a Galerkin method [54] to find limiting cases and predict critical values of R and k for the instability. The numerical calculations done by means of the shooting method along with the graphics corresponding to the marginal curves are given in Section 5. In Section 6, the experimental data [27] are compared with the numerical results. A discussion is given in the final section.

2. Equations of motion

We consider an infinite horizontal layer of a suspension of gyrotactic microorganisms. The fluid layer is bounded at $z^* = -H,\ 0$. The fluid where the cellular microorganisms swim is water with density ρ. Each cell has a volume υ and density $\rho + \Delta\rho$, where $\Delta\rho \ll \rho$. The suspension is considered dilute and incompressible. Density fluctuations in the suspension are small enough such that the Boussinesq approximation is valid and the corresponding governing equations are

$$\rho\frac{D\mathbf{u}^*}{Dt^*} = -\nabla p^* - n^*\upsilon g\Delta\rho\mathbf{k} + \mu\nabla^2\mathbf{u}^* \tag{1}$$

$$\frac{\partial n^*}{\partial t^*} = -\nabla\cdot\mathbf{J}^* \tag{2}$$

$$\nabla\cdot\mathbf{u}^* = 0 \tag{3}$$

where t^* is the time, $\mathbf{u}^*$ is the suspension velocity, p^* is the pressure, $g\mathbf{k}$ is the acceleration due to gravity, $\mathbf{k}$ is the vertical unit vector, μ is the viscosity, n^* is the concentration of microorganisms, and $\mathbf{J}^*$ is the flux density of organisms through the fluid defined as

$$\mathbf{J}^* = n^*\mathbf{u}^* + n^*V_c\mathbf{p}^* - D_c\nabla n^* \tag{4}$$

where V_c is the cell swimming speed, $\mathbf{p}^*$ is a unit vector representing the average orientation of cells, and D_c is a scalar microorganism mass diffusion coefficient independent of the other parameters of the problem. Use is made of Cartesian coordinates with the z-axis in the vertical direction. The walls at $z^* = -H,\ 0$ are considered to be rigid. As pointed out by Hill et al. [24] although the top boundary is open to the air, algal cells tend to collect at the surface forming what appears to be a packed layer, and it is unlikely that the boundary is ever fully stress-free. Then the boundary conditions are

$$\mathbf{u}^* = 0 \,\text{at}\, z^* = -H, 0 \tag{5}$$

$$\mathbf{J}^* \cdot \mathbf{k} = 0 \,\text{at}\, z^* = -H, 0 \tag{6}$$

In the basic state, the fluid velocity is zero and $n^* = n_0^*(z)$ and $\mathbf{p}_0 = \mathbf{k}$. Thus for $n_0^*(z)$ from Eq. (2) with the boundary conditions (6), we have

$$n_0^*(z) = \frac{\overline{n} V_c H \exp\left[V_c z^*/D_c\right]}{D_c(1 - \exp\left[-V_c H/D_c\right])} \tag{7}$$

where $\overline{n}$ represents the average concentration of organisms. Eq. (7) is the same basic state as presented by Ghorai and Hill [48, 49] whose linear stability will be investigated. It differs from that of Childress et al. [19] and Hill et al. [24] by the coefficient

$$\frac{V_c H}{D_c(1 - \exp\left[-V_c H/D_c\right])}$$

3. Linear stability

We make the governing Eqs. (1–3) nondimensional by scaling all lengths with H, the time with H^2/D_c, the fluid velocity with D_c/H, the pressure with $\nu D_c \rho/H^2$, and the cell concentration with $\overline{n} H V_c/D_c$. Now the dimensionless variables are expressed without star. The boundaries are located at $z = -1, 0$ and the basic state is

$$\mathbf{u_0} = 0, \quad \mathbf{p_0} = \mathbf{k}, \quad n_0(z) = \frac{e^{dz}}{1 - e^{-d}}$$

where the nondimensional quantity $d = V_c H/D_c$ is the ratio of swimming speed of microorganisms and their representative mass diffusion velocity. Here, d is called the motility of the microorganisms. In order to investigate the linear stability of the system, small perturbations have to be considered. They are

$$\mathbf{u} = \mathbf{u}_0 + \delta\mathbf{u}_1, \quad p = p_0 + \delta\mathbf{p}_1, \quad \mathbf{p} = \mathbf{p}_0 + \delta\mathbf{p}_1, \quad n = n_0 + \delta n_1$$

where $\delta \ll 1$. The components of $\mathbf{u^1}$ are (u_1, v_1, w_1). In this way, the nondimensional governing Eqs. (1–3) are linearized to order $O(\delta)$. Then, we have the following linear equations

$$Sc^{-1} \frac{\partial \mathbf{u}_1}{\partial t} = -\nabla p - R n_1 \mathbf{k} + \nabla^2 \mathbf{u}_1 \tag{8}$$

$$\frac{\partial n_1}{\partial t} = -w_1 \frac{dn_0}{dz} - d\frac{\partial n_1}{\partial z} - dn_0 \nabla \cdot \mathbf{p_1} + \nabla^2 n_1 \tag{9}$$

$$\nabla \cdot \mathbf{u_1} = 0 \tag{10}$$

where

$$S_c = \frac{\nu}{D_c}, \quad R = \frac{\overline{n} \upsilon g \Delta\rho H^3 d}{D_c \nu \rho}$$

are the Schmidt and bioconvection Rayleigh numbers, respectively. Pedley and Kessler [55] give a definition of the vector $\mathbf{p_1}$ for swimming microorganisms with spheroidal shape. They determine $\mathbf{p_1}$ in terms of $\mathbf{u_1}$ that in nondimensional form is

$$\mathbf{p_1} = G\left[(1+\alpha_0)\frac{\partial \mathbf{u_{1\perp}}}{\partial z} - (1-\alpha_0)\nabla_\perp w_1\right] \tag{11}$$

$$G = \frac{BD_c}{H^2} \tag{12}$$

where the subscript $\perp$ denotes the horizontal component, α_0 is the cell eccentricity, and G is the nondimensional form of the gyrotactic orientation parameter B. Finally after substitution of $\mathbf{p_1}$ and n_0, the governing equations become

$$\mathrm{Sc}^{-1}\frac{\partial \mathbf{u}}{\partial t} = -\nabla p - Rn\mathbf{k} + \nabla^2\mathbf{u} \tag{13}$$

$$\frac{\partial n}{\partial t} = \frac{de^{dz}}{1-e^{-d}}\left(-w + G\left[(1+\alpha_0)\frac{\partial^2 w}{\partial z^2} + (1-\alpha_0)\nabla_\perp^2 w\right]\right) - d\frac{\partial n}{\partial z} + \nabla^2 n \tag{14}$$

$$\nabla \cdot \mathbf{u} = 0 \tag{15}$$

with boundary conditions

$$\mathbf{u} = 0 \,\text{at} z = -1, 0 \quad \text{and} \quad \frac{\partial n}{\partial z} - dn = 0 \,\text{at} z = -1, 0 \tag{16}$$

where the superscripts have been deleted. Notice that the adimensionalization of the equations is different from that of Hill et al. [24]. Here, an application of a more general asymptotic analysis for any magnitude of d is used. An analytic Galerkin method and a shooting numerical method for the solution of the proper value problem allowed us to have an interesting perspective of the stability of the present problem under research. The results are used here to compare with the experimental data of the flagellated alga *Chlamydomonas nivalis*.

By elimination of the pressure from Eqs. (13–15), it is possible to obtain a coupled system of two equations, for w and n, to describe the instability of the system. The perturbations of the variables will be analyzed in terms of normal modes of the form

$$w = W(z)\exp\left[\left(k_x x + k_y y\right)i + \sigma t\right],$$
$$n = \Phi(z)\exp\left[\left(k_x x + k_y y\right)i + \sigma t\right]$$

where $k = \sqrt{k_x^2 + k_y^2}$ is the wavenumber of the disturbance and σ is the growth rate. The wavenumber is scaled as $k = k^* H$ corresponding to a nondimensional wavelength $\lambda = 2\pi/k$. Thus, the governing equations become

$$-Rk^2\Phi = \left(\frac{\sigma}{S_c} + k^2 - D^2\right)\left(k^2 - D^2\right)W \tag{17}$$

$$\left(\sigma + dD + k^2 - D^2\right)\Phi = \frac{de^{dz}}{1-e^{-d}}\left(-1 + G\left[(1+\alpha_0)D^2 - (1-\alpha_0)k^2\right]\right)W \tag{18}$$

subject to the boundary conditions

$$W = DW = D\Phi - d\Phi = 0 \;\text{ at }\; z = -1, 0 \tag{19}$$

where $D = d/dz$. The variables of the above problem can be changed in order to simplify the analysis. The change of dependent variable is

$$\Phi = F(z)e^{dz}$$

Then, Eqs. (17) and (18) and the boundary conditions Eq. (19) become

$$-Rk^2Fe^{dz} = \left(\frac{\sigma}{S_c} + k^2 - D^2\right)\left(k^2 - D^2\right)W \tag{20}$$

$$\left(\sigma - dD + k^2 - D^2\right)F = \frac{d}{1 - e^{-d}}\left(-1 + G\left[(1 + \alpha_0)D^2 - (1 - \alpha_0)k^2\right]\right)W \tag{21}$$

subject to the new boundary conditions

$$W = DW = DF = 0 \text{ at } z = -1, 0 \tag{22}$$

In this form, the equations are very similar to those of the well-known problem of thermal convection in an infinite horizontal fluid layer between nonconducting boundaries [50–53, 56]. The familiar fixed heat flux boundary condition is the main characteristic of those thermal convection problems and is analogous to that presented in Eq. (22). The equations derived by Childress et al. [19] can also be analyzed from the present view point of this change of variable. In the theory of thermal convection as in that of Childress et al. [19], a zero critical wavenumber is found as a result of the fixed flux boundary condition. In more recent models, which include the effects of gyrotaxis, the similarity with the thermal convection problem is not valid unless $G = 0$.

4. Asymptotic analysis

In this section, the eigenvalue problem stated in the system of Eqs. (13–15) with boundary condition Eq. (16) is investigated by means of two analytic methods. The magnitude of the marginal value of R is a function of all the other parameters. The way in which the solution of the stability problem is to be carried out is as follows. For a given value of d and G, we must determine the lowest value for R with respect to the wavenumber k. The values obtained are the critical Rayleigh numbers R_c at which instability will first occur.

4.1 Asymptotic analysis

We conducted a general asymptotic analysis in comparison with those used before [19, 24, 26] which included the restrictions of the limits $d \ll 1$ for shallow layers and $d \gg 1$ for deep layers along with different restrictions for G. In a similar way, as in other problems of convection, we follow the steps of Chapman and Proctor [51], Dávalos-Orozco [52], and Dávalos-Orozco and Manero [53]. Under the above conditions, the analysis is very complex, the reason why use has been made of the Maple algebra package. Thus, we look for a solution to Eqs. (20) and (21) using the following expansions:

$$W = W_0 + \varepsilon W_1 + ..., \tag{23}$$

$$\Phi = \Phi_0 + \varepsilon\Phi_1 + ..., \tag{24}$$

$$R = R_0 + \varepsilon R_1 + ..., \tag{25}$$

$$\sigma = \varepsilon\sigma_0 + \varepsilon^2\sigma_1 + ... \tag{26}$$

where $\varepsilon \ll 1$. We also consider no restrictions for d and G and rescale the wavenumber as $k = \varepsilon^{1/2}\tilde{k}$. Thus, after substitution of expansions Eqs. (23–26) and

the mentioned scalings in Eqs. (20) and (21) with boundary condition Eq. (22), we obtain the following systems of equations at different orders.

At order $O(1)$

$$D^4W_0 + \tilde{k}^2 R_0 e^{dz} F_0 = 0, \tag{27}$$

$$\left(D^2 + d\right)F_0 = 0 \tag{28}$$

subject to

$$W_0 = DW_0 = DF_0 = 0 \text{ at } z = -1, 0. \tag{29}$$

At order $O(\varepsilon)$

$$D^4W_1 - \left(2\tilde{k}^2 + \frac{\sigma_0}{Sc}\right)D^2W_0 + \tilde{k}^2 e^{dz}(R_0F_1 + R_1F_0) = 0, \tag{30}$$

$$\frac{d}{1-e^{-d}}\left[G(1+\alpha_0)D^2 - 1\right]W_0 - \left(\sigma_0 + \tilde{k}^2\right)F_0 + \left(D^2 + d\right)F_1 = 0 \tag{31}$$

subject to

$$W_1 = DW_1 = DF_1 = 0 \text{ at } z = -1, 0. \tag{32}$$

At order $O(\varepsilon^2)$

$$D^4W_2 - \left(2\tilde{k}^2 + \frac{\sigma_0}{Sc}\right)D^2W_1 + \left(\tilde{k}^4 + \frac{\sigma_0\tilde{k}^2}{Sc} - \frac{\sigma_1}{Sc}D^2\right)W_0 + \tilde{k}^2 e^{dz}(R_0F_2 + R_1F_1 + R_2F_0) = 0, \tag{33}$$

$$\frac{d}{1-e^{-d}}\left\{\left[G(1+\alpha_0)D^2 - 1\right]W_1 - G(1+\alpha_0)\tilde{k}^2W_0\right\} - \left(\sigma_0 + \tilde{k}^2\right)F_1 - \sigma_1F_0 + \left(D^2 + d\right)F_2 = 0 \tag{34}$$

subject to

$$W_2 = DW_2 = DF_2 = 0 \text{ at } z = -1, 0. \tag{35}$$

The systems of equations at order $O(\varepsilon)$ and higher are inhomogeneous and must satisfy their corresponding solvability conditions allowing to compute the Rayleigh number R as an eigenvalue in terms of the other parameters of the problem. Solvability conditions are found as usual [57]: each inhomogeneous system is multiplied by the solution to the adjoint of the homogeneous system and integrated over the range of the independent variable. The resulting integral must vanish.

Thus, the solvability conditions at $O(\varepsilon)$ and $O(\varepsilon^2)$ are, respectively,

$$0 = \frac{d}{1-e^{-d}}\int_{-1}^{0} e^{dz}\left[G(1+\alpha_0)D^2 - 1\right]W_0 dz - \left(\sigma_0 + \tilde{k}^2\right)\int_{-1}^{0} e^{dz}F_0 dz \tag{36}$$

$$\begin{aligned} 0 = {} & \frac{d}{1-e^{-d}}\int_{-1}^{0} e^{dz}\left\{\left[G(1+\alpha_0)D^2 - 1\right]W_1, -G(1+\alpha_0)\tilde{k}^2W_0\right\}dz \\ & -\left(\sigma_0 + \tilde{k}^2\right)\int_{-1}^{0} e^{dz}F_1 dz - \sigma_1\int_{-1}^{0} e^{dz}F_0 dz \end{aligned} \tag{37}$$

The solutions of the system of equations at leading order are

$$F_0 = 1, \quad W_0 = f_1(z,d)R_0\tilde{k}^2 \tag{38}$$

where the function $f_1(z,d)$ can be obtained from the authors upon request. For convenience, the solution F_0 has been normalized to 1. The next step is to evaluate the solvability condition Eq. (36) at $O(\varepsilon)$ and obtain an expression for σ_0

$$\sigma_0 = \tilde{k}^2\left\{\left[1 - d^2G(1+\alpha_0)\right]A_0R_0 - 1\right\} \tag{39}$$

The constant A_0 is large and can be obtained from the authors upon request. At order $O(\varepsilon)$ similar steps as those for solving the system of equations at $O(1)$ are followed to find F_1 and W_1. Then, algebraically F_1 is

$$F_1 = \left[G(1+\alpha_0)f_2(z,d) + f_3(z,d)\right]R_0\tilde{k}^2 \tag{40}$$

After substitution of F_0, W_0, F_1, and σ_0 into Eq. (30), the velocity W_1 can be calculated subject to its corresponding boundary condition Eq. (32). Because of the term e^{dz} appearing in the system of equations at $O(1)$, the expression of W_1 is very large and complicated and will not be given here. The evaluation of the solvability condition at order $O(\varepsilon^2)$ given in Eq. (37) yields

$$\begin{aligned}\sigma_1 = {} & \left[1 - d^2G(1+\alpha_0)\right]\tilde{k}^2A_0R_1 - \left\{\left[G^2(1+\alpha_0)^2A_1 + G(1+\alpha_0)A_2 + A_3\right]R_0^2\right. \\ & + G(1-\alpha_0)A_4R_0 + R_0\left[1 - d^2G(1+\alpha_0)\right]\{[G(1+\alpha_0)A_5 + A_6]R_0 \\ & \left. + A_7 + \left(\left[1 - d^2G(1+\alpha_0)\right]A_8R_0 + A_7/2\right)/Sc\right\}\tilde{k}^4\end{aligned} \tag{41}$$

The growth rate can now be obtained by substitution of σ_0 and σ_1 into the expansion for σ given in Eq. (26). However σ is omitted to save space but can be obtained from the authors upon request. Finally, use is made of the expansion Eq. (25) for R.

Now, the transition from stability to instability via a stationary state is investigated by setting $\sigma = 0$. Thus, the corresponding value of R for the marginal state is

$$\begin{aligned}R = {} & \frac{1}{\left[1 - d^2G(1+\alpha_0)\right]A_0} + \frac{k^2}{\left[1 - d^2G(1+\alpha_0)\right]A_0} \\ & \left\{\frac{G(1-\alpha_0)}{\left[1 - d^2G(1+\alpha_0)\right]} + \frac{G(1+\alpha_0)A_5 + A_6}{\left[1 - d^2G(1+\alpha_0)\right]A_0^2} + \frac{G^2(1+\alpha_0)^2A_1 + G(1+\alpha_0)A_2 + A_3}{\left[1 - d^2G(1+\alpha_0)\right]^2A_0^2} + \frac{A_7}{A_0}\right\}\end{aligned} \tag{42}$$

where some simplifications have been made with the use of R_0 obtained from Eq. (39). The functions $f_2(z,d)$ and $f_3(z,d)$ and the coefficients A_1 to A_8 appearing in the above expressions are functions of d and can be obtained from the authors upon request. The result for R_0 is

$$R_0 = \frac{1}{\left[1 - d^2G(1+\alpha_0)\right]A_0} \tag{43}$$

From the expression for the Rayleigh number given in Eq. (42), it is possible to calculate the limit for $d \ll 1$. In this case, we consider d and k to be of the same order in such a way that $k_d = k/d$ and $k_d \sim O(1)$. Then, under these assumptions, the approximation of $R(k,d,G,\alpha_0)$ is

$$R = 720\left\{1 + d^2\left[\frac{17}{420} + G(1+\alpha_0) + k_d^2\left(\frac{17}{462} - \frac{2}{7}G(5-2\alpha_0)\right)\right]\right\} + O(d^3) \quad (44)$$

Here we point out that in the present chapter, our definition of the Rayleigh number differs from that defined by Hill et al. [24]. If our approximation given in Eq. (44) is multiplied by $\frac{d}{1-e^{-d}} = \left(1 + d/2 + d^2/12 - d^4/720...\right)$, the same approximation by Hill et al. [24] is obtained. Moreover, if $G = 0$ this becomes that given by Childress et al. [19]. In the more general expression of R for a small wavenumber approximation, Eq. (42) has a special characteristic due to its dependence on the square of the wavenumber k. The first coefficient at zeroth order in k corresponds to R_0, and that at the second order in k is R_1. Even though in the experiments on bioconvection [27], only finite critical wavenumbers $k_c > 0$ have found these coefficients are very useful. For example, it can be shown from R_0 that if $A_0 > 0$ and

$$1 - d^2G(1+\alpha_0) > 0 \quad (45)$$

then $R_0 < 0$. This corresponds to a stable stratification, which is not the case here. The second coefficient R_1 in Eq. (42) is a very important result, because it provides information about the shape of the marginal curve with respect the critical wavenumber. That information can be obtained by making zero the coefficient R_1 and calculating the following critical value of the gyrotaxis number G_c

$$\begin{aligned} 0 = {} & G^2(1+\alpha_0)^2\left[A_1 - d^2A_5 - d^2A_0^2\frac{1-\alpha_0}{1+\alpha_0}\right] + G(1+\alpha_0) \\ & \left[A_2 + A_5 - d^2(A_6 + A_7A_0) + A_0^2\frac{1-\alpha_0}{1+\alpha_0}\right] + A_3 + A_6 + A_7A_0 \end{aligned} \quad (46)$$

From this equation, two admissible cases are possible when Eq. (45) is satisfied. First, for fixed values of d, α_0, and $G > G_c$, the marginal curve starts at $k = 0$ and then decreases monotonically. However, according to the numerical analysis presented below, the marginal curves in fact first decrease and then start to grow monotonically after a minimum is attained, at the critical wavenumber. In the second case, for fixed values of d, α_0, and $G < G_c$, the marginal curves start at $k = 0$ and then grow monotonically. Here, the critical wavenumber is always zero. The importance of these results is that the magnitude of G_c agrees very well with the results of the marginal curves found in the numerical analysis given below. This critical value determines the magnitude for which the curves have a finite critical wave number ($G > G_c$) or a zero critical wavenumber ($G < G_c$). It is of interest to note that some of the magnitudes of the gyrotaxis parameter G calculated from the data in the literature are very near but above of G_c. This is the reason why some of the curves found from numerical analysis are almost flat in a range of wavenumbers near to zero. Because the experimental critical wavenumbers found for gyrotactic bioconvection are always finite, we conclude that G_c is important to point out where to find the theoretical limitations of the model.

4.2 Analytic Galerkin method

Here use is made of the analytical Galerkin method to study the eigenvalue problem of Eqs. (17)–(18) with the boundary condition Eq. (19). This method has been used before by Pellew and Soutwell [58], Chandrasekhar [54], and Gershuni and Zhukovitskii [59]. Even though this is an approximate method, it has a very high precision. The advantage of the method is that it is possible to obtain an explicit expression of the Rayleigh number R. Here, it is supposed that $\sigma = 0$.

Briefly, the method consists in assuming a trial function which satisfies the boundary conditions for each of the dependent variables. Let that variable be Φ which after substitution in one of the equations of the problem allows for the exact solution of the other variables, let us say W. Both trial functions are now substituted into the other coupled equation. Then, use is made of the orthogonality properties of the solutions in this equation to obtain the proper value of the Rayleigh number as a function of the other parameters [60].

In this way, the proposed expansions of Φ and W are

$$\Phi = \sum_{n=0}^{\infty} B_n \exp(dz)\cos \pi n z \quad \text{and} \quad W = \sum_{n=0}^{\infty} B_n W_n \tag{47}$$

then, after substitution of Φ of Eq. (47) into Eq. (20), W_n is the solution of the following differential equation:

$$\left(D^2 - k^2\right)^2 W_n = -Rk^2 \exp(dz)\cos \pi n z \tag{48}$$

which is subjected to the conditions

$$W_n = DW_n = 0 \ \text{ at } \ z = -1.0. \tag{49}$$

The solution is

$$W_n = (a_1 \cos \pi n z + a_2 \sin \pi n z)e^{dz}k^2 R + c_1 e^{kz} + c_2 e^{-kz} + c_3 z e^{kz} + c_4 z e^{-kz} \tag{50}$$

where c_1 to c_4 are constants of integration which can be found by evaluating in the boundary condition Eq. (49).

Next, Eq. (18) is multiplied by Φ and is integrated in the range $z = -1$ to $z = 0$, to get

$$\begin{aligned} &\frac{d}{1-e^{-d}} \int_{-1}^{0} \Phi\left(-1 + G\left[(1+\alpha_0)D^2 - (1-\alpha_0)k^2\right]\right) W dz \\ &- \int_{-1}^{0} \Phi\left[D\left(e^{-dz}D\right) - k^2 e^{-dz}\right]\Phi dz = 0 \end{aligned} \tag{51}$$

After substitution of Φ and W, given in Eqs. (47) and (50) and some simplifications, we obtain

$$\begin{aligned} &\left| \frac{d}{1-e^{-d}} \int_{-1}^{0} \Phi_m\left(-1 + G\left[(1+\alpha_0)D^2 - (1-\alpha_0)k^2\right]\right) W_n dz \right. \\ &\left. - \int_{-1}^{0} \Phi_m\left[D\left(e^{-dz}D\right) - k^2 e^{-dz}\right]\Phi_n dz \right| = 0 \end{aligned} \tag{52}$$

This determinant, calculated with the help of the software Maple, is the solvability condition from which the eigenvalue R is calculated. The resulting algebraic expression of the integrals in this equation is very complex and will not be presented here. However, the first approximation of R, corresponding to the element (0,0) of the matrix in the determinant Eq. (52), is

$$R = \frac{\left(1 - e^{-d}\right)A_{10}}{de^{-d}\left[1 + G(1-\alpha_0)k^2 - d^2 G(1+\alpha_0)\right]A_9} \tag{53}$$

where A_9 and A_{10} are functions of the wavenumber k and d and can be obtained from authors upon request. This result is new because it includes, for the first time,

all the parameters of the problem without any approximation. In the limit of $d, k, G \to 0$, R reduces to the well-known value of 720. Higher-order estimates of R can be obtained from Eq. (52), which provides a useful check on numerical calculations. The comparison of R given in Eq. (42), obtained from the asymptotic analysis, and that of Eq. (52) shows that in the limit $k \to 0$, the agreement was very good.

5. Numerical computations by a shooting method

Here, the shooting method [61] is used to solve the eigenvalue problem posed by the system of Eqs. (20) and (21) subjected to the boundary condition Eq. (22). Curves of marginal stability in the plane (k, R) were calculated for fixed values of the parameters d, G, and α_0. Notice that very good agreement was always found among the values of the R of the asymptotic analysis (in the limit $k \to 0$), of the Galerkin method, and of the numerical computations. Calculations were made in two ways. First, the parameters d, G, and α_0 were varied in order to obtain a representative set of marginal curves for the problem of bioconvection. Second, experimental data were also used to fix the values of d, G, and α_0 and used to find theoretical values of k_c and R_c that could be compared with their corresponding experimental values. Here, in particular, a selection is made of $\alpha_0 = 0.4$, which corresponds to the flagellated alga *Chlamydomonas nivalis*. **Figures 1–3** show marginal curves for different values of the gyrotaxis parameter G, while d remains fixed with magnitudes 0.1, 1, and 5, respectively. These figures clearly show the effect the gyrotaxis parameter G has on the critical wavenumber. When the magnitude of G is large enough, the critical wavenumber changes from zero to a finite value which increases with G, as shown by the squares located at the minimum value of R. Notice that it is found that the critical value G_c, which represents the magnitude at which the properties of the marginal curves change, from having $k_c = 0$ to $k_c > 0$, is very well approximated by Eq. (46). This critical value is important because it represents the magnitude of G below which the present theory ceases to predict the experimental results which always show critical wavenumbers $k_c > 0$.

In the curves shown in **Figure 1a–b**, the critical values of the gyrotaxis parameter are $G_c = 0.0306, 0.0266, 0.0060$, respectively. As mentioned above for $G > G_c$, the critical wavenumber is finite, and for $G < G_c$ the critical wavenumber is always zero. The combined effects of the velocity of the swimming of microorganisms, d,

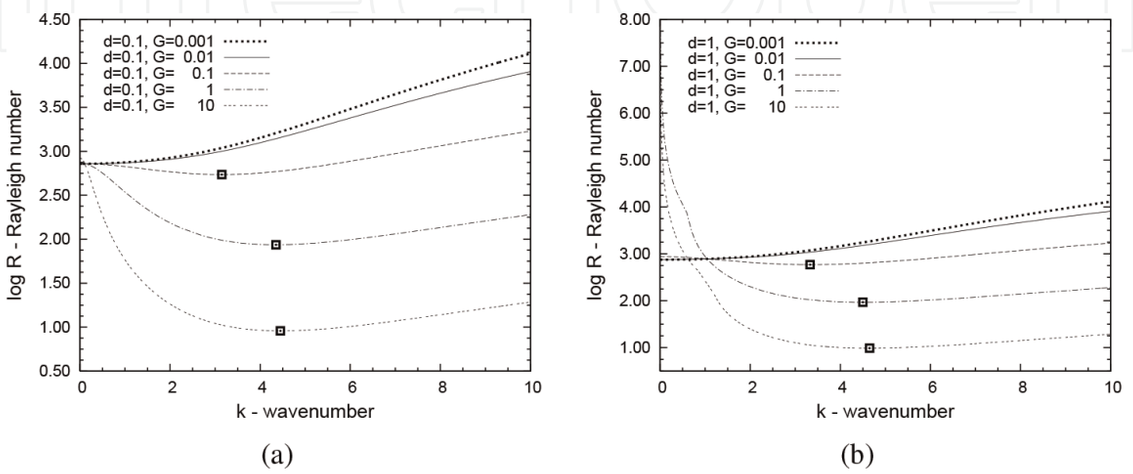

Figure 1.
(a) Graphs of log R vs. k for fixed $d = 0.1$. (b) Graphs of log R vs. k for fixed $d = 1$. The black square markers indicate the position of the critical wavenumber and Rayleigh number.

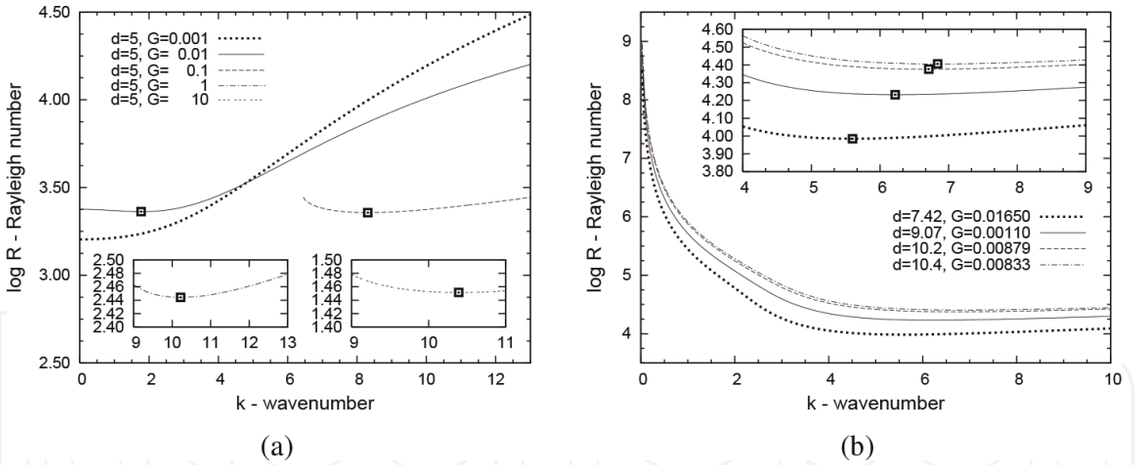

Figure 2.
(a) Graphs of log R vs. k for fixed $d = 5$. (b) Graphs of log R vs. k for experiments 35, 2, 4, and 9 with d increasing from the curve below to above. The black square markers indicate the position of the critical wavenumber and Rayleigh number.

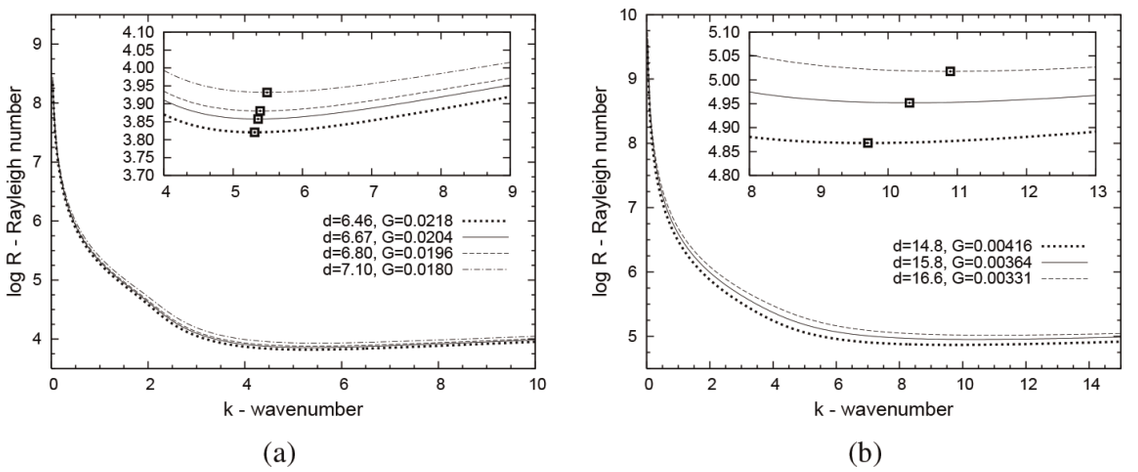

Figure 3.
(a) Graphs of log R vs. k for experiments 26–29, 24, 31, and 16 with d increasing from the curve below to above. (b) Graphs of log R vs. k for experiments 13, 10, and 20 with d increasing from the curve below to above. The black square markers indicate the position of the critical wavenumber and Rayleigh number.

and that of gyrotaxis, G, change the location of the critical wavenumber. Note also that for fixed d, when G increases, the system becomes more unstable. From the **Figure 1a** and **b**, it can be seen that the most unstable case corresponds to that for $d = 0.1$ and $G = 10$ where $k_c = 4.45$ and $R_c = 9.0618$. This may be understood by the fact that the accumulation of microorganisms near to the top of a shallow layer is faster than in a deeper one. This is due to the important role that the mass diffusion of microorganism D_c and the depth of suspension H play on the instability of the system. The value of G_c in the limit of $d, k \to 0$ can also be calculated from Eq. (46) by means of an asymptotic analysis. That is,

$$G_c = \frac{17}{132(5 - 2\alpha_0)} + O(d^2) \tag{54}$$

Here, some theoretical curves are presented of which some have a very good agreement and others a reasonable agreement with the experiments 2, 4, 9, 10, 13, 16, 20, 24, 26, 27, 28, 29, 31, and 35, performed by Bees and Hill [27].

The values for the motility d and the gyrotaxis parameter G used in **Figures 2** and **3** were calculated based on experimental data by Bees and Hill [26, 27], which

	Experimental results			Theoretical predictions					Error (%)	
EN	d_{BH}	k_c	R_{BHc} $(\times 10^6)$	d_{BH}	$d_{BH^2\eta}$	α_0	k_c	R_{BHc} $(\times 10^6)$	k	R_{BH}
2	44.7	5.11	3.25	40	16	0.2	51	5.0	898	53
				40	16	0.4	51	9.0	898	176
23	204	7.84	863	200	32	0.2	270	1700	3343	96

EN represents the experiment name. Subscript BH indicates that the definition of Bees and Hill, [26] for the parameters d and R is used. η is the gyrotactic parameter [26].

Table 1.
Experimental measurements of Bees and Hill [27] and their theoretical prediction [26].

in here are presented in **Tables 2** and **3** of the following section. In order to observe in detail the position of the critical point (k_c, R_c) in **Figures 2** and **3**, a local magnification is included.

Here, a comparison is done of our theoretical results of (k_c, R_c) with the theoretical ones presented by Bees and Hill [26] in their Table VI. According to Bees and Hill [26], experiments 2 and 23 in their Table V have (k_c, R_c) of comparable order with those in their Table VI. In our **Table 1**, we reproduce the comparison made by Bees and Hill [26] of their own theoretical and experimental results of their Table V, and we added the corresponding error in percent of the wavenumbers and Rayleigh numbers, respectively. Note that the value $\alpha_0 = 0.4$ corresponds to flagellated microorganisms such as *Chlamydomonas nivalis*, while $\alpha_0 = 0.2$ corresponds to nonflagellated. Notice that their experimental and theoretical values of d are not exactly the same.

For the sake of comparison of our theoretical results with those of the experiments, **Table 1** shows the percent of error calculated by taking the difference of the experimental and theoretical values and then dividing by the smallest one. In **Table 1**, the more realistic value $\alpha_0 = 0.4$ for *Chlamydomonas nivalis* is included, which corresponds to the second line of experiment 2 of Bees and Hill [26] predictions. It is clear from **Table 3** that our theoretical results show a very important improvement in the reduction of the percent error with respect to experiment 2.

6. Comparison with experiments

In this section a comparison is done of our theoretical results of R_c and k_c with the corresponding experimental values obtained by Bees and Hill [27]. Here use is made of the results of the 39 experiments shown in Table I of Bees and Hill [27]. Besides, the more realistic value of the parameter $\alpha_0 = 0.4$, corresponding to the flagellated algae *Chlamydomonas nivalis*, is also used to calculate d, G, and R.

In **Table 3**, the values of d, G, and R resulting from the experimental data are presented. Note in **Table 2** that the experimental results of the cell swimming speed V_s and of the cell diffusivity D_c are given inside a range of values. In this case, a particular value inside the range has to be selected. The swimming speed used here is $63\times10^{-4} cm/s$. The decision is based on the results obtained by Hill and Hader [62], Pedley and Kessler [25], and Bees and Hill [26]. The value of the cell diffusivity was decided to be that corresponding to an average over the range given in **Table 2**, that is, $D_c = 27.5 \times 10^{-5} cm^2/s$.

Very recent experimental measurements on the diffusivity for different microorganisms like the biflagellated alga *Chlamydomonas reinhardtii* have been reported

by Polin et al. [63]. Bees and Hill [27] state that there is some evidence to suggest that cells of *Chlamydomonas nivalis* are not gyrotactic during the first week of subculturing; then if it is not the case for the cells of *Chlamydomonas reinhardtii*, more measurements for the parameters α_0, B, V_s, H, $\overline{n}$, and k_c would be needed in order to perform comparison between theoretical and experimental results. The definitions of d, G, and R are related with those of Bees and Hill [26] d_{BH}, η, and R_{BH}, respectively, as follows:

$$d = \frac{V_s^2 \tau K_2}{D_c K_1} d_{BH}, \quad G = \frac{D_c}{V_s^2 \tau} \eta, \quad R = \frac{K_2^2 \tau^3 V_s^5}{D_c^2 H K_1^2} \left(1 - \exp\left[-\frac{K_1 H}{K_2 V_s \tau}\right]\right) R_{BH} \tag{55}$$

where the constants $K_2 = 0.15$ and $K_1 = 0.57$ (see [26] for more details). τ is a direction correlation time which equals $1.3s$ in the nonflagellated case and $5s$ in the flagellated case. The data corresponding to the suspension depth H and the average cell concentration of microorganisms $\overline{n}$ of each experiment (see [27] for more details) have not been reported in **Table 3**. Only the parameters d, G, k, and R are presented in that table. It is also found that the value of the G of each experiment is greater (but sometimes near) than their corresponding critical value G_c of Eq. (46). Under these conditions, all the critical wavenumbers have to be $k_c > 0$.

By using the data of our **Table 2** and Table I of Bees and Hill [27], the experimental values for d, G, and R_E were calculated and listed in **Table 3**. The experimental value of the wavenumber k_E was also obtained from Table I of Bees and Hill [27] and was calculated as follows: the wavelength $\lambda_0(cm)$ is nondimensionalized with the corresponding suspension depth $H(cm)$ to get λ_E, and then the critical wavenumbers were calculated from $k_E = 2\pi/\lambda_E$. R_T and k_T are our theoretical wavenumber and Rayleigh number obtained by the shooting method. The curves of marginal stability corresponding to experimental results with good and very good agreement with theory are shown in **Figures 2** and **3**. As explained above, we have a substantial improvement in the agreement of the critical wavenumbers and Rayleigh numbers with respect to the experimental results (see **Table 3**). A great number of experimental data have been compared with the present theory in **Table 3**.

Name	Description	Value
ϑ	Cell volume	5×10^{-10} cm^3
g	Acceleration due to gravity	10^3 cms^{-2}
D_c	Cell diffusivity	5×10^{-5}–5×10^{-4} cm^{2}s^{-1}
ρ	Fluid density	1 gcm^{-3}
$\rho + \Delta\rho$	Cell density	1.05 gcm^{-3}
ν	Kinematic viscosity	10^{-2} cms^{-2}
V_c	Cell swimming speed	0–2×10^{-2} cms^{-1}
B	Dimensional gyrotaxis parameter	3.4 s
B	Including flagella	6.3 s
α_0	Cell eccentricity	0.20–0.31
α_0	Including flagella	0.4

Table 2.
Estimates and measurements of typical parameters for a suspension of the alga Chlamydomonas nivalis *[24, 25, 64, 65].*

NE	d	$G \times 10^{-2}$	RE	RT	kE	kT	Error k (%)	Error R (%)
1	7.63	1.56	7043.64	10384.23	5.67	5.65	0.353	47.6
2	9.07	1.10	10599.14	17075.28	5.12	6.22	21.5	61.1
3	8.36	1.30	23319.62	13531.06	8.59	5.95	44.4	72.3
4	10.2	0.879	24835.78	23783.25	5.96	6.71	12.6	4.42
5	11.9	0.636	12433.03	37984.11	6.81	7.69	12.9	205
6	16.7	0.326	59993.82	105787.08	6.61	10.9	64.9	76.3
7	9.14	1.09	4676.34	17544.33	6.01	6.31	4.99	275
8	8.73	1.19	7198.47	15309.02	7.25	6.09	19.0	112
9	10.4	0.833	20618.78	25437.60	8.33	6.84	21.8	23.4
10	15.8	0.364	88709.37	89546.43	8.34	10.3	23.5	0.943
11	6.46	2.18	3700.78	6613.53	5.24	5.31	1.33	78.7
12	12.1	0.621	39993.68	40261.72	5.66	7.94	40.3	0.670
13	14.8	0.416	77622.32	73779.00	7.85	9.71	23.7	5.20
14	8.80	1.17	8561.41	15655.83	6.93	6.11	13.4	82.9
15	7.28	1.71	4022.37	9146.74	5.46	5.54	1.46	127
16	7.10	1.80	6960.80	8540.98	6.43	5.49	17.1	22.7
17	10.7	0.788	18965.81	27708.92	4.16	7.02	68.7	46.1
18	10.7	0.788	18965.81	27708.92	8.32	7.02	18.1	46.1
19	10.7	0.788	18965.81	27708.92	4.89	7.02	43.5	46.1
20	16.6	0.331	107793.38	104192.94	8.7	10.9	25.3	3.45
21	8.80	1.17	8561.41	15655.83	7.01	6.11	14.7	82.9
22	8.13	1.37	6910.81	12466.94	6.11	5.84	4.62	80.4

NE	d	$G \times 10^{-2}$	RE	RT	kE	kT	Error k (%)	Error R (%)
23	10.7	0.791	41777.52	27799.28	7.84	7.06	11.0	50.3
24	6.67	2.04	6260.75	7202.62	6.07	5.36	13.2	15.0
25	4.26	5.01	1044.17	2301.46	6.22	4.82	29.0	120
26	6.46	2.18	5663.12	6613.53	6.71	5.31	26.4	16.8
27	6.46	2.18	5663.12	6613.53	6.05	5.31	13.9	16.8
28	6.46	2.18	5663.12	6613.53	5.37	5.31	1.13	16.8
29	6.46	2.18	5663.12	6613.53	5.94	5.31	11.9	16.8
30	7.83	1.48	33599.24	11220.81	7.46	5.74	30.0	199
31	6.80	1.96	6478.07	7585.38	6.00	5.39	11.3	17.0
32	4.47	4.56	4519.70	2583.99	6.66	4.86	37.0	74.9
33	2.70	12.4	475.88	2180.73	4.97	6.52	31.2	358
34	3.85	6.14	1958.29	4879.03	6.21	6.46	4.02	149
35	7.42	1.65	8259.40	9655.91	6.15	5.60	9.82	16.9
36	7.83	1.48	33599.24	11220.81	6.49	5.74	13.1	199
37	5.22	3.33	2418.53	3794.61	6.37	4.99	27.6	56.9
38	6.87	1.92	20572.53	22011.51	10.4	7.13	46.0	6.99
39	6.87	1.92	20572.53	22011.51	10.8	7.13	51.9	6.99

EN means experiment name, and subscripts E and T indicate experimental and theoretical data. Cell eccentricity $\alpha_0 = 0.4$ *is used.*

Table 3.
Experimental measurements of wavenumbers [27] and present theoretical predictions.

Some numerical results agree very well with experiments, as can be seen in the experiments 4, 10, 12, 13, 20, and 35 of **Table 3**. Others are good, such as the results of experiments 9, 16, 24, 26, 27, 28, 29, and 31. With respect to the other data in **Table 3**, it might be possible that if the experimental measurements are improved, the agreement with theory will be better. The results given here show that the approximate and numerical solutions of the system of governing equations presented in this paper may bring a light to the solution of many other problems of bioconvection.

7. Conclusions

The governing equations of bioconvection were used to investigate the problem of an infinite horizontal microorganism suspension fluid layer. The theoretical predictions of the critical wavenumber k_c and Rayleigh number R_c were compared with their experimental counterparts [27]. Very good, good, and fair agreements were found. But in general, we may say that our numerical results improve by far those obtained by Bees and Hill [26].

With the asymptotic analysis for $k << 1$, it was possible to calculate a Rayleigh number not reported before without any restrictions on the magnitudes of d and G. This result is important because it was also possible to calculate a critical value of the gyrotaxis parameter G_c which indicates the boundary between the possibility of a marginal curve with $k_c = 0$ $(G < G_c)$ and another one with $k_c > 0$ $(G > G_c)$.

However, it is clear from the experimental results that the critical wavenumbers are finite and large and that the former case is not physical. Therefore, this G_c also defines the limit of validity of the theory. Note that it agrees very well with numerical analysis.

An analytic Galerkin method was also used to obtain a general expression of R without any restriction on the magnitudes of d, G, and $k \sim O(1)$. This gave us an explicit expression of R not reported before which proved to be very useful when checking with the numerical computations.

Numerical results have shown that the system becomes more unstable when the layers are shallow. The physical interpretation of such situation is that the accumulation of microorganisms near the top of the layer in the shallow case is faster than in the deeper case, due to the smaller depth of suspension H. A consequence of this is that the critical wavenumber is smaller for shallower layers. This can be explained by means of the boundary conditions of the microorganism concentration. If the parameter d tends to zero, the boundary conditions tend to those similar to the "fixed heat flux" boundary conditions of the problem of natural convection heated from below [50–53, 56]. Moreover, it has been shown above that by a change of variable, it is possible to transform the boundary conditions of the concentration into those similar to the "fixed heat flux" boundary conditions. In that problem it has been shown that the critical wavenumber tends to zero. However, due to the gyrotaxis, the critical wavenumber is not zero in the present problem if $G > G_c$, which, from the experimental results, is the case here. But notice in **Figures 1–3** that in fact, also in this case, the critical wavenumber decreases with a decrease of d. The change of the critical wavenumber with respect to G is also clear in the figures. The critical wavenumber decreases with a decrease of G.

Finally, we would like to point out that it is our hope that the results presented in this chapter may stimulate researchers to make more new and precise experiments on bioconvection in the near future.

Nomenclature

B	dimensional gyrotactic parameter, s
k	wavenumber
D_c	cell diffusivity, cm^2s^{-1}
d	motility of microorganisms
G	dimensionless gyrotactic parameter
g	acceleration due to gravity, cms^{-2}
H	layer depth, cm
$\mathbf{J}^*$	flux density of organisms
$\overline{n}$	average cell concentration
n^*	concentration of microorganisms
p	pressure
R	Rayleigh number
Sc	Schmidt number
t^*	time
V_c	cell swimming speed, cms^{-1}
$\mathbf{u}^*$	fluid velocity
$\mathbf{x}^*$	Cartesian coordinates
Greek symbols	
α_0	cell eccentricity
μ	viscosity, $gcm^{-1}s^{-1}$
ν	kinematic viscosity, cm^2s^{-1}
ρ	water density, gcm^{-3}
ϑ	cell volume, cm^{-3}
Subscripts	
BH	result obtained by Bees and Hill [26]
c	critical value
E	experimental result
T	theoretical result

Acknowledgements

The authors would like to thank Alberto López, Alejandro Pompa, Cain González, Raúl Reyes, Ma. Teresa Vázquez, and Oralia Jiménez for technical support. I. Pérez Reyes would like to thank the Programa de Mejoramiento del Profesorado (PROMEP).

Author details

Ildebrando Pérez-Reyes[1*] and Luis Antonio Dávalos-Orozco[2]

1 Facultad de Ciencias Químicas, Universidad Autónoma de Chihuahua, Chihuahua, Mexico

2 Departamento de Polímeros, Instituto de Investigaciones en Materiales, Universidad Nacional Autónoma de México, México, D.F., México

*Address all correspondence to: ildebrando3@gmail.com

References

[1] Noever DA, Matsos HC. A Biosensor for Cadmium Based on Bioconvective Patterns. Nasa tm–103523, NASA; 1990

[2] Itoh A, Toida H, Saotome Y. Control of bioconvection and its application for mechanical system: 2nd report, pitch optimization of electrodes array and driving of mechanical system by controlled bioconvection. Transactions of the Japan Society of Mechanical Engineers. Part B. 2006;**72**(716):972-978

[3] Kawaguchi T, Itoh A, Toyoda Y. Control of bioconvection and its mechanical application: 4th report: Generation of upward flow and its position control. Transactions of the Japan Society of Mechanical Engineers. Part B. 2002;**2002**(14):317-318

[4] Itoh A, Toida H, Saotome Y. Control of bioconvection and its application for mechanical system: 1st report basic effects of electrical field on bioconvection. Transactions of the Japan Society of Mechanical Engineers. Part B. 2001;**67**(662):2449-2454

[5] Itoh A, Toida H. Control of bioconvection and its mechanical application. In: 2001 IEEE/ASME International Conference on Advanced Intelligent Mechatronics. Proceedings; 2001. pp. 1220-1225

[6] Itoh A. Motion control of protozoa for bio mems. IEEE/ASME Transactions on Mechatronics. 2000;**5**(2):181-188

[7] Itoh A, Tamura W. Object manipulation by a formation-controlled Euglena group. In: Bio-mechanisms of Swimming and Flying. Kato Bunmeisha, Japan: Springer Japan; 2008. pp. 41-52

[8] Itoh A, Tamura W, Mishima T. Motion control of Euglena group by weak laser scanning system and object manipulation using Euglena group. In: 2005 IEEE/ASME International Conference on Advanced Intelligent Mechatronics. Proceedings. 2005. pp. 43-47

[9] Kim D, Brigandi S, Kim P, Kim MJ. Control of tetrahymena pyriformis as a microrobot. In: Microbiorobotics. Oxford, UK: Elsevier; 2012. pp. 277-287

[10] Kim DH, Brigandi S, Julius AA, Kim MJ. Real-time feedback control using artificial magnetotaxis with rapidly-exploring random tree (RRT) for *Tetrahymena pyriformis* as a microbiorobot. In: 2011 IEEE Int. Conf. Robotics Autom. IEEE; May 2011

[11] Ceylan H, Giltinan J, Kozielski K, Sitti M. Mobile microrobots for bioengineering applications. Lab on a Chip. 2017;**17**(10):1705-1724

[12] Magariyama Y, Kudo S, Goto T, Takano Y. An engineering perspective on swimming bacteria:high-speed flagellar motor, intelligent flagellar filaments, and skillful swimming in viscous environments. In: Bio-mechanisms of Swimming and Flying. Japan: Springer; 2004. pp. 1-12

[13] Itoh A. Euglena motion control by local illumination. In: Bio-mechanisms of Swimming and Flying. Japan: Springer; 2004. pp. 13-26

[14] Platt JR. Bioconvection patterns in cultures of free-swimming organisms. Science. 1961;**133**:1766-1767

[15] Pedley TJ, Kessler JO. Hydrodynamic phenomena in suspensions of swimming microorganisms. Annual Review of Fluid Mechanics. 1992;**24**:313-358

[16] Hill NA, Pedley TJ. Bioconvection. Fluid Dynamics Research. 2005;**37**:1-20

[17] Murase M. Dynamics of Cellular Motility. West Sussex, England: John Wiley and Sons; 1992

[18] Häder R, Hemmersbach D-P, Lebert M. Gravity and the Behavior of Unicellular Organisms. New York, USA: Cambridge University Press; 2005

[19] Childress M, Levandowsky S, Spiegel EA. Pattern formation in a suspension of swimming microorganisms: Equations and stability theory. Journal of Fluid Mechanics. 1975;**63**:591-613

[20] Harashima A, Watanabe M, Fujishiro I. Evolution of bioconvection patterns in a culture of motile flagellates. Physics of Fluids. 1988;**31**(4): 764-775

[21] Dávalos-Orozco LA, del Castillo LF. Hydrodynamic behavior of suspensions of polar particles. In: Encyclopedia of Surface and Colloid Science. New York, USA: Taylor and Francis; 2006. pp. 2798-2820

[22] Dávalo-Orozco LA. Natural convection in a polar suspension with internal rotation. Revista Mexicana de Física. 2002;**48**(S1):31-37

[23] Pedley TJ, Hill NA, Kessler JO. The growth of bioconvection patterns in a uniform suspension of gyrotactic micro–organisms. Journal of Fluid Mechanics. 1988;**195**:223-237

[24] Hill NA, Pedley TJ, Kessler JO. Growth of bioconvection patterns in a suspension of gyrotactic micro-organisms in a layer of finite depth. Journal of Fluid Mechanics. 1989;**208**: 509-543

[25] Pedley TJ, Kessler JO. A new continuum model for suspensions of gyrotactic micro-organisms. Journal of Fluid Mechanics. 1990;**212**(1):155-182

[26] Bees MA, Hill NA. Linear bioconvection in a suspension of randomly swimming, gyrotactic micro-organisms. Physics of Fluids. 1998; **10**(8):1864-1881

[27] Bees MA, Hill NA. Wavelength of bioconvection patterns. The Journal of Experimental Biology. 1997;**200**: 1515-1526

[28] Loeffer JB, Mefferd RB. Concerning pattern formation by free-swimming microorganisms. The American Naturalist. 1952;**86**:325-329

[29] Fornshell JA. An experimental investigation of bioconvection in three species of microorganisms. The Journal of Protozoology. 1978;**25**(1):125-133

[30] Kessler JO. Co-operative and concentrative phenomena of swimming microorganisms. Contemporary Physics. 1985;**26**(2):147-166

[31] Dombrowski C, Cisneros L, Chatkaew S, Goldstein RE, Kessler JO. Self-concentration and large-scale coherence in bacterial dynamics. Physical Review Letters. 2004;**93**(9): 2277-2282

[32] Tuval I, Cisneros L, Dombrowski C, Wolgemuth CW, Kessler JO, Goldstein RE. Bacterial swimming and oxygen transport near contact lines. Proceedings of the National Academy of Sciences of the United States of America. 2005;**102**:098103

[33] Akiyama A, Ookida A, Mogami Y, Baba SA. Spontaneous alteration of the pattern formation in the bioconvection of Chlamydomonas reinhardtii. Journal of the Japan Society of Microgravity Application. 2005;**22**(4):210-215

[34] Ishikawa T, Simmonds MP, Pedley TJ. Hydrodynamic interaction of two swimming model micro-organisms. Journal of Fluid Mechanics. 2006;**568**: 119-160

[35] Ishikawa T, Pedley TJ. Diffusion of swimming model micro-organisms in a semi-dilute suspension. Journal of Fluid Mechanics. 2007;**588**:437-462

[36] Ishikawa T, Pedley TJ. The rheology of a semi-dilute suspension of swimming model micro-organisms. Journal of Fluid Mechanics. 2007;**588**:399-435

[37] Ishikawa T, Locsei JT, Pedley TJ. Development of coherent structures in concentrated suspensions of swimming model micro-organisms. Journal of Fluid Mechanics. 2008;**615**:401-431

[38] Ishikawa T, Yamaguchi T, Pedley TJ. Bio-Mechanisms of Swimming and Flying, chapter Properties of a semi-dilute suspension of swimming microorganisms, pages 17–28. Springer Japan, Kato Bunmeisha, Japan, 2008.

[39] Kitsunezaki S, Komori R, Harumoto T. Bioconvection and front formation of *Paramecium tetraurelia*. Physical Review E. 2007;**76**:046301

[40] Mogami Y, Baba SA. Amplified expression of the gravity effect on the spatio-temporal formation of bioconvection pattern. In: Proceedings of the Twenty-Fourth Space Utilization Symposium. Vol. 24; 2008. pp. 264-266

[41] Mogami Y, Ookida A, Baba SA. Bioconvection as a research model of gravitational biology. In: Proceedings of the Twenty-First Space Utilization Symposium. Vol. 21; January 2005. pp. 213-215

[42] Mogami Y, Yamane A, Gino A, Baba SA. Bioconvective pattern formation of tetrahymena under altered gravity. The Journal of Experimental Biology. 2004; **207**:3349-3359

[43] Sawai S, Mogami Y, Baba SA. Cell proliferation of *Paramecium tetraurelia* on a slow rotating clinostat. Advances in Space Research. 2007;**39**:1166-1170

[44] Mogami Y, Akiyama A, Baba SA. Comparative physiology of bioconvection. In: Proceedings of the Twenty-Second Space Utilization Symposium. Vol. 22; January 2006. pp. 222–223

[45] Takeda A, Mogami Y, Baba SA. Gravikinesis in Paramecium: Approach from the analysis on the swimming behavior of single cells. Biological Sciences in Space. 2006;**20**(2):44-47

[46] Mogami Y, Ishii J, Baba SA. Theoretical and experimental dissection of gravity-dependent mechanical orientation in gravitactic microorganisms. The Biological Bulletin. 2001;**201**:26-33

[47] Itoh A, Amagai K, Arai M, Mifune H. The effect of rotational gravitational field on bioconvection pattern. Transactions of the Japan Society of Mechanical Engineers. Series B. 1999; **65**(630):698-705

[48] Ghorai S, Hill NA. Development and stability of gyrotactic plumes in bioconvection. Journal of Fluid Mechanics. 1999;**400**:1-31

[49] Ghorai S, Hill NA. Periodic arrays of gyrotactic plumes in bioconvection. Physics of Fluids. 2000;**12**(1):5-22

[50] Pismen LM. Inertial effects in long-scale thermal convection. Physics Letters A. 1986;**116**(5):241-244

[51] Chapman CJ, Proctor MRE. Nonlinear Rayleigh–Bénard convection between poorly conducting boundaries. Journal of Fluid Mechanics. 1980; **101**(4):759-782

[52] Dávalos-Orozco LA. Magnetoconvection in a rotating fluid between walls of very low thermal conductivity. Journal of the Physical Society of Japan. 1984;**53**(7):2173-2176

[53] Dávalos-Orozco LA, Manero O. Thermoconvective instability of a second-order fluid. Journal of the Physical Society of Japan. 1986;**55**(2): 442-445

[54] Chandrasekhar S. Hydrodynamic and Hydromagnetic Stability. New

York, USA: Dover Publications, Inc.; 1981

[55] Pedley TJ, Kessler JO. The orientation of spheroidal micro-organisms swimming in a fluid flow field. Proceedings of the Royal Society of London. Series B. 1987;**231**(1262): 47-70

[56] Gertsberg VL, Sivashinsky GI. Large cells in nonlinear Rayleigh–Bénard convection. Progress in Theoretical Physics. 1981;**66**(4):1219-1229

[57] Nayfeh AH. Introduction to Perturbation Techniques. New York, USA: John Wiley and Sons, Inc.; 1981

[58] Pellew A, Soutwell RV. On maintained convective motion in a fluid heated from below. Proceedings of the Royal Society of London. Series A. 1940; **176**(966):313-343

[59] Gershuni GZ, Zhukovitskii EM. Convective Instability of Incompressible Fluids. Jerusalem, Israel: Keter Publications; 1976

[60] Finlayson AB. The Method of Weighted Residuals and Variational Principles. Mathematics in Science and Engineering. New York, USA: Academic Press; 1972

[61] Press WH, Teukolsky SA, Vetteling WT, Flannery BP. Numerical Recipes. The Art of Scientific Computing. 3rd ed. Cambridge, USA: Cambridge University Press; 2007

[62] Hill NA, Häder D-P. A biased random walk model for the trajectories of swimming micro-organisms. Journal of Theoretical Biology. 1997;**186**:503-526

[63] Polin M, Tuval I, Drescher K, Gollub JP, Goldstein RE. Chlamydomonas swims with two gears in a eukaryotic version of run-and-tumble locomotion. Science. 2009;**325**(24):487-490

[64] Kessler JO. Individual and collective fluid dynamics of swimming cells. Journal of Fluid Mechanics. 1986;**173**: 191-205

[65] Jones MS, Le Baron L, Pedley TJ. Biflagellate gyrotaxis in a shear flow. Journal of Fluid Mechanics. 1994;**281**: 137-158